This article has been accepted for publication in a future issue of this journal, but has not been fully edited. Content may change prior to final publication. Citation information: DOI 10.1109/TVT.2019.2897899, IEEE Transactions on Vehicular Technology

Automotive Traction Inverters: Current Status and Future Trends

John Reimers, *Student Member, IEEE,* Lea Dorn-Gomba, *Student Member, IEEE,* Christopher Mak, *Student Member, IEEE,* and Ali Emadi, *Fellow, IEEE*

***Abstract*—Traction inverters are crucial components of modern electrified automotive powertrains. Advances in power electronics have enabled lower cost inverters with high reliability, efficiency and power density, suitable for mass market consumer automotive applications. This paper presents an independent review of the state-of-the-art traction inverter designs from several production vehicles across multiple manufacturers. Future trends in inverter design are identified based on industry examples and academic research. Wide bandgap devices and trends in device packaging are discussed along with active gate driver implementations, current and future trends in system integration, and advanced manufacturing techniques.**

***Index Terms*—Automotive applications, Electric vehicles, Electrified powertrains, Hybrid electric vehicles, Inverters, Power electronics, Traction motor drives, Transportation electrification**

I. Introduction

ELECTRIFIED vehicles (EVs) are continuing to show promise as more manufacturers announce plans to develop electrified models in order to improve fuel economy and remain competitive as consumer demands shift towards efficient, cleaner vehicles. These include hybrid electric vehicles (HEVs), plug-in hybrid electric vehicles (PHEVs), battery electric vehicles (BEVs), and fuel cell vehicles. At the heart of all electrified powertrains is one or more electric machines (EMs) which operate either in conjunction with an internal combustion engine (ICE) or replace it entirely. The EMs found in EVs today are most commonly of the AC permanent magnet (PM) or AC induction machine (IM) type [1, 2]. To drive them, a traction inverter is required to convert the direct current available from the battery pack to variable frequency alternating current. In addition to the motoring mode, the machines can also operate as generators, requiring the inverter to act as a rectifier and return energy to the battery.

In 2012, the U.S. Department of Energy (DOE) initiated a long term project called the 'EV Everywhere Grand Challenge' with the goal of defining a technology roadmap for cost-effective, powerful and reliable EVs that can compete with conventional ICE vehicles [3]. National laboratories, original equipment manufacturers (OEMs), and suppliers are working together to improve the power electronics systems subjected to aggressive targets for 2020 as a part of the technology roadmap. Regarding the inverter objectives, a 30 kW continuous (55 kW peak) design is expected to achieve a power density of 13.4 kW/L and a specific density of 14.1 kW/kg at a cost of \$3.3/kW for 100 000 units. Delphi Technologies and the DOE overcame some of the barriers and disclosed in a 55 kW peak traction inverter with 15 kW/L and 17 kW/kg [4]. However the cost remains the biggest challenge as the inverter reached \$5/kW. Several OEMs have achieved a subset of the goals as well, and traction inverter design will be discussed in detail in the following sections. The DOE recently updated the objectives to accelerate the integration of EVs in the market and defined new targets for 2025 [5]. For the inverter power module composed of an inverter and, if applicable, a DC/DC boost converter, a 100 kW integrated design with 100 kW/L at \$2.7/kW is expected. This represents 18% cost reduction and 87% volume reduction compared to the 2020 goals. In view of these new targets, major technological breakthroughs are required.

While previous reviews have either covered the entire electrified powertrain [6] or focused on theoretical aspects of the inverter [7], the goal of this paper is to present a thorough review of the production inverter implementations across several vehicle manufacturers. In the following, a review of current production automotive traction inverters with a focus on BEVs and PHEVs is presented. BEVs and PHEVs tend to have higher power inverters and, as the industry trends towards fully electric powertrains, the majority of traction inverters in the future will be in the 100-500 kW range compared to the 30-60 kW range found in HEVs today. Finally, future trends are identified based on ongoing research and emerging industry practices.

II. Inverter Design

A. Topology

Due to their high efficiency and low cost, the vast majority of production EVs today utilize three phase voltage source inverters (VSI) based on insulated gate bipolar transistors (IGBTs). As shown in Fig. 1, the battery pack can be either directly connected to the inverter DC input (Fig. 1a), or a DC/DC boost converter can be used to step up the battery voltage and supply the inverter with a controlled DC voltage (Fig. 1b). In both circuits, a large DC-link capacitor C_{dc} smooths the ripple current and voltage generated by the switching action of the active devices. This ensures a nearly constant DC-link

Manuscript received October 19, 2018; revised December 30, 2018; accepted January 29, 2019. *(Corresponding author: John Reimers)*

The authors are with the McMaster Institute for Automotive Research and Technology (MacAUTO), McMaster University, Hamilton, ON L8S 4L8, Canada (e-mail: reimerja@mcmaster.ca; dorngoml@mcmaster.ca; makcs@mcmaster.ca; emadi@mcmaster.ca)

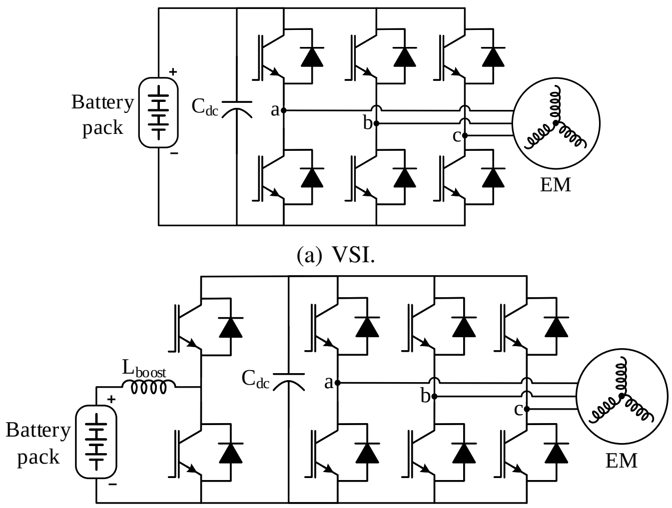

(b) VSI combined with a DC/DC boost converter.

Fig. 1: Standard inverter topologies used in the automotive industry.

voltage and reduces the high frequency current harmonics. The boost converter is commonly implemented with two switching devices such that it is bidirectional and can return energy to the battery during regenerative braking. The topology can be scaled to higher power levels by paralleling multiple converter phases, which has the benefit of reducing ripple if interleaving control is used. The VSI topology requires six switches which are modulated to generate a three phase sinusoidal output current to the EM [8].

Thanks to its single stage conversion, the architecture shown in Fig. 1a is cheap, easy to manufacture and requires simple control of the switching devices. Moreover, the VSI has been intensively studied and widely used in the industry over the past decades which makes this topology mature, robust, and reliable.

B. Alternative candidates

Many alternative topologies have been suggested, however most of them require additional power switches and passive elements beyond the standard VSI which increases not only the cost, but also the control complexity, volume and weight of the system. Extensions of the two level VSI and accompanying modulation schemes have also been proposed such as the H8 architecture [9] and four-leg inverters [10]. These topologies can reduce the high frequency common mode voltage variation within the EM which is known to cause bearing failure [11].

1) Current source inverter (CSI): The CSI is a traditional inverter that converts power from a DC current source to an AC output [8]. A DC voltage source, such as a battery pack, can also be used if it is connected in series with a large inductor. The circuit is composed of six switching devices with bidirectional voltage blocking and unidirectional current flow capability. Thus, symmetric thyristors or IGBTs in series with diodes are common solutions implemented in the industry. For motor drive applications, capacitor filters are required on the AC output due to the high distortion of the line currents caused by the switching action.

One advantage of the CSI is its capability of boosting the input voltage to produce an AC output with a higher peak value than the DC input voltage. This eliminates the need for a separate DC/DC boost converter and extends the constant power range of the EM by providing sufficient output voltage even as the machine's back EMF rises above the DC-link [12].

While the significant reduction of the DC link capacitor can improve the power density of the CSI, there is still a need for a DC-link inductor that is usually bulky and heavy in high power applications. Practically, the lower efficiency and higher cost compared to the VSI have prevented adoption of the CSI in automotive traction applications [13].

2) Z-source inverter (ZSI): The ZSI combines some characteristics of the VSI and CSI where either a voltage or current source can be directly connected to its input terminals [14]. The circuit uses six semiconductor devices that require unidirectional voltage blocking capability and bidirectional current flow. With appropriate control of the switches, the ZSI can operate as a buck-boost inverter since it is capable of producing an AC output voltage either higher or lower than the DC input source.

The ZSI could be a suitable alternative solution for electrified powertrain applications due to its buck-boost feature since DC sources, such as batteries, provide a widely varying voltage range [15, 16]. The ZSI provides higher or similar efficiency than the VSI and the combination of the VSI with a DC/DC boost converter respectively [17]. However, even though the number of active devices is low, the passive component requirements are higher in the ZSI. Hence, the cost and volume of this topology still prevents its adoption by the automotive industry.

3) Three-level inverters: Over the past few years, three-level inverters have gained interest in the industry as alternative solutions to the standard VSI. Among the many topologies that have been developed, the Neutral Point Clamped (NPC) and the T-type NPC (TNPC) are the most competitive solutions [18–20].

Advanced studies have highlighted several aspects of the benefits of three-level inverters [21, 22]. An efficiency comparison for a wide range of switching frequencies has been conducted to compare the VSI, the NPC and the TNPC inverters. Results show that the efficiency of the VSI is higher only for low frequencies but drops significantly above 10 kHz. On the other hand, the TNPC is more efficient for medium frequencies between 10 kHz to 30 kHz, while the NPC becomes slightly more efficient for frequencies above 30 kHz. Three-level inverters provide output voltages with lower harmonic distortion than the VSI, reducing the EMI filter requirements and improving the efficiency of the motor. Nevertheless, the capacitor banks for three-level inverters have a volume twice that of the VSI and requires additional control to ensure capacitor voltage balancing. Moreover, both topologies suffer from high cost and increased control complexity due to a high part count.

This article has been accepted for publication in a future issue of this journal, but has not been fully edited. Content may change prior to final publication. Citation information: DOI 10.1109/TVT.2019.2897899, IEEE Transactions on Vehicular Technology

C. Modulation techniques

The AC output voltages produced by the inverter and feeding the EM are generated through pulse width modulation (PWM) techniques that switch the power semiconductors in a desired pattern. Closed-loop control is achieved by the inverter through phase current and rotor position feedback, thus requiring at least two phase current sensors in the inverter and a suitable interface for a resolver or encoder from the EM.

1) Sinusoidal PWM (SPWM): SPWM is one of the most classic techniques used in the industry due to its simplicity [23]. It was first developed with analog circuits but digital implementation is now a standard procedure. One drawback of this modulation scheme is its limited use of the DC-link voltage V_{dc} since the maximum amplitude of the fundamental output phase voltage is $V_{dc}/2$. Moreover, this method generates relatively high total harmonic distortion (THD) in the line voltages compared to other techniques, causing higher harmonic losses.

2) Space Vector PWM (SVPWM): Despite its more intensive computational requirements, SVPWM has gained popularity as the widespread adoption of digital signal processors (DSPs) and microcontrollers has enabled low cost implementations [23, 24]. SVPWM achieves better performance by generating reduced THD compared to SPWM, improving the efficiency of the inverter as well as the EM. Furthermore, the maximum fundamental amplitude of the phase voltage is equal to $V_{dc}/\sqrt{3}$, which is about 15% higher than SPWM method in the linear region [25, 26]. Hence, the SVPWM enables a better DC link utilization, which can be even further extended through six-step operation in the over modulation region.

3) Six-step modulation: Though it is challenging to confirm which modulation strategy is used for the traction inverters in every EV, it is believed that SVPWM is preferred due to its performance superiority. For example, it has been reported in [27, 28] that General Motors (GM) employs SVPWM for the linear modulation region and then applies six-step modulation in the over modulation region.

The six-step mode, also known as square-wave modulation, is named after the six distinct steps the output phase voltages take over a fundamental cycle [29]. During the six-step mode, the DC link voltage utilization is maximized since the fundamental amplitude of the phase voltage is equal to V_{dc}. This improves the EM performance by increasing the torque capability in the flux-weakening region. On the other hand, this method raises some practical issues due to low-order current harmonics that make control of the torque challenging. The six-step modulation remains a complementary method combined with another PWM technique due to its lack of output voltage amplitude control.

D. Inverter components

IGBTs have been the predominant choice for traction inverters compared to other switching devices. This is due to the maturity of the technology, its wide availability, low cost, and sufficient power capability. Indeed, IGBTs with a blocking voltage of 650V to 1200V can easily handle today's battery pack voltages which vary from 200V to 450V in most EVs. Furthermore, power modules with high current capability or discrete devices connected in parallel have emerged as solutions in response to higher power demands.

Gate drivers are greatly responsible for the efficiency of the inverter as they influence the dynamic behavior of the IGBTs and the freewheeling diodes. They are composed of integrated circuits (ICs) that transmit isolated control signals to switch the device and provide protective feedback. For high voltage applications, such as traction inverters, optocouplers or pulse transformers are typically used for isolation [30]. The gate driver design needs to consider the factors influencing the power device switching performance. Several approaches have been developed, from passive circuits using external gate-emitter capacitors and gate resistors to closed-loop control that adjusts the gate drive output based on the IGBT operation [31].

To implement the motor control software, a microcontroller or DSP is included, typically on a dedicated control board within the inverter. Given the computational requirements of the motor control and modulation schemes, 32-bit floating-point processors clocked at over 100 MHz are the norm for traction inverters. As control algorithms continue to increase in complexity and switching speeds rise, it has been suggested that field programmable gate array (FPGA) hardware be used to implement the modulation while the DSP handles the motor control, in order to improve timing accuracy and reduce the DSP requirements [32, 33]. A position sensor is typically used to determine the rotor angle of the EM. Most automotive applications use a resolver and a dedicated resolver-to-digital (R2D) chip is included on the inverter control board to provide the necessary excitation signals as well as the analog to digital conversion of the resolver signal.

Current sensors are used to measure the inverter's AC ouput current, which is fed back to the DSP which implements the closed loop control. For automotive applications, open loop Hall effect sensors are typically applied due to their relatively low cost, high bandwidth and inherent isolation.

The DC-link capacitor is a crucial component of the inverter as it protects both the input source and the power devices from large current and voltage spikes. Hence, the proper selection is based on the ripple current requirements and the capacitance calculated from voltage ripple requirements [34, 35]. Compared to electrolytic capacitors, film capacitors have shown many benefits for inverter applications where high current ripple capability is a concern while high capacitance is less important. Indeed, a more power-dense, efficient, and low cost design can be achieved with film capacitors, as shown in [36]. Moreover, while the temperature variation affects both technologies, electrolytic capacitors are particularly sensitive, with every $10\,^{\circ}\mathrm{C}$ rise in operating temperature reducing the lifetime of the capacitor by approximately half [37].

As power requirements for traction inverters continue to rise, heat dissipation has become a critical concern in inverter design. In fact, high temperatures have been identified as the primary source of failure and overheating dramatically reduces the reliability and lifetime of power converters [38, 39]. Hence, thermal management systems, such as heat sinks, have become staple components and optimizing their design is a challenging task as they require advanced loss and thermal models [40–

43]. Many cooling techniques have been studied over the years [44]. Liquid cooling is usually preferred in high power inverters since they efficiently dissipate more heat in a limited space compared to forced air cooling. They also operate better regardless of the ambient environmental conditions.

Busbars are commonly used in high power inverters due to their superior current capability compared to printed circuit boards (PCBs) and higher power density compared to the use of wires. Their design is a complex procedure that requires many considerations such as the shapes of the DC-link capacitor and power devices, the thermal management system, the current density, and the operating environment. Particular attention must be paid to minimize any parasitic inductance introduced by the busbar connections which can have a significant effect on surge voltages during switching events [45].

III. Current status

Numerous OEMs now offer electrified or fully electric models. Information on the implementations of the inverters for these vehicles is either published in technical papers by the manufacturers and their suppliers, or it is obtained through reverse engineering by private or governmental organizations. The rated power and power densities of the reviewed traction inverter implementations are summarized in Table I.

A. General Motors (GM)

GM has had a long history of electrification, beginning with the EV1 in 1996. Their first generation traction inverter featured a power density of 3 kW/L [6]. Today they offer several electrified models and have published technical papers on some of the inverter designs with their Tier 1 supplier Delphi Technologies.

1) Chevrolet MY2016 Volt: The 2016 model year Chevrolet Volt marks the second generation of GM's first production PHEV. The traction inverter is described in detail in [46] and [47]. The inverter features dual VSIs for the traction and generator machines with power ratings of 87 kW and 48 kW respectively, as well as a smaller VSI to drive the variable speed oil pump for the ICE. The maximum DC link voltage is 430 V and the maximum total simultaneous AC power for both inverters is reported as 180 kVA with a power density of 17.3 kVA/L. While the first generation Volt inverter was situated separately in the engine bay, the second generation is located directly on the transmission manifold to eliminate the need for phase cables. This tighter integration of the inverter with the powertrain reduces component count, harness complexity and assembly cost while improving collision robustness.

The overall layout of the inverter is shown in Fig. 2. The double-sided cooling (DSC) IGBT power module developed by Delphi Technologies is used for both the motor and generator inverters. Wire bonds were eliminated in favor of solderable interconnects to improve reliability and reduce inductance. The coefficient of thermal expansion (CTE) of the ceramic substrates was matched to that of the silicon to further increase reliability. The twelve modules are soldered in two rows of six to a power PCB which is connected to the DC-link from above

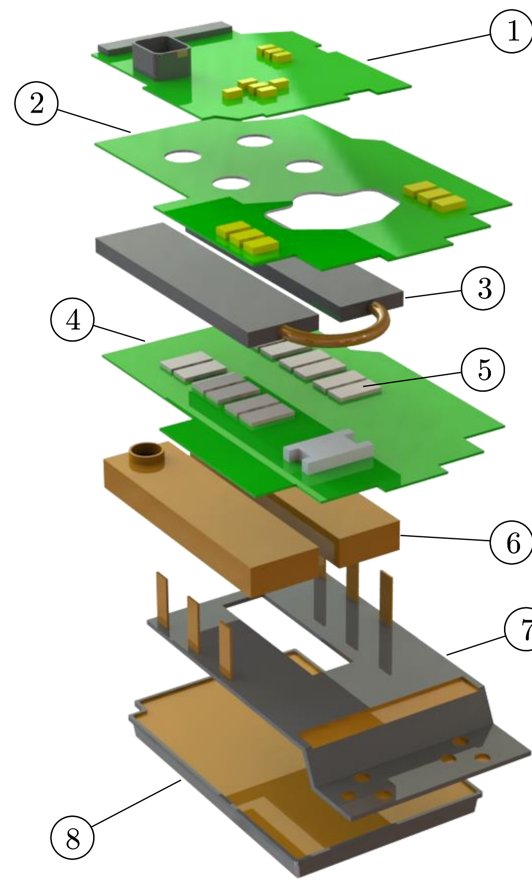

Fig. 2: Second generation Chevrolet Volt inverter components [46]: 1) Control board 2) Gate driver board 3) Top heat sink 4) Power board 5) DSC IGBT modules 6) Bottom heat sink 7) Phase busbars 8) DC-link capacitor.

in the center. The AC output bus bar assembly connects from below to the edges of the PCB. The DC-link capacitor sits below the AC bus bar and connects upwards in the center to the DC link on the power board.

Cooling of the IGBT modules is achieved with copper metal injected molded heat sinks. With the elimination of phase cables, the AC output bus bars are now connected directly to the EMs which offers a direct path for heat flow from the EM windings to the inverter power modules. An additional cooling mechanism consisting of an electrically insulated thermal interface material and stamped aluminum sheet was required to divert heat flow from the bus bars to the inverter housing.

2) Cadillac MY2016 CT6: The Cadillac CT6 PHEV builds upon the Volt powertrain design to meet the higher performance requirements of a luxury rear wheel drive application. The traction inverter is described in [48] and [49], again featuring dual VSIs for the motor and generator, and a third smaller VSI for the engine oil pump. Despite the identical topology, the implementation is somewhat different from the Volt. AC phase cables to the motors remain, likely for packaging reasons given the larger ICE and longitudinal orientation of the hybrid transmission.

The power switches are phase leg modules developed by Hitachi which feature direct cooling. The module packaging eliminates any thermal grease, with water ethylene glycol (WEG) coolant passing directly over both sides of the module. An aluminum pin fin plate is attached to each side of the die with an electrically insulating sheet allowing the module to be immersed in coolant, resulting in a reported 35% reduction in thermal impedance from junction to coolant. The modules are directly connected via bus bars to the DC-link capacitor, which is also liquid cooled. The increased efficiency and reduced thermal impedance of the IGBT modules enable a compact design which was required to meet the packaging constraints for the large hybrid powertrain.

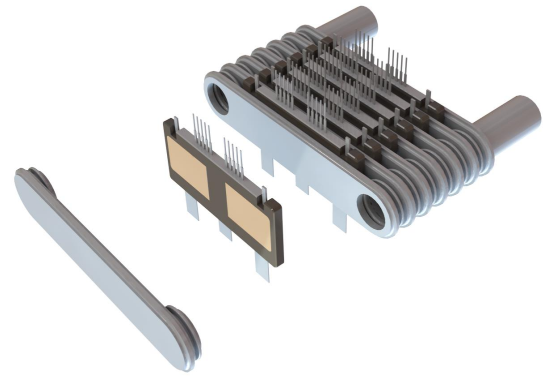

Fig. 3: Toyota "power card" DSC IGBT module stack with heat exchanger [51].

B. Toyota MY2016 Prius

Toyota has long been at the forefront of mass market HEVs since the introduction of the Prius in 1997. They continue to focus on hybrid models with some expansion in to PHEVs with the Prius Prime in 2012. Significant reverse engineering efforts have been undertaken by Oak Ridge National Laboratory (ORNL) on the 2004 and 2010 model year Prius [50]. Toyota has also published technical papers on the development of the Prius inverter, most recently for the fourth generation model [51].

The fourth generation Prius was launched in North America in early 2016. Toyota has integrated two VSIs, a DC/DC boost converter, and a DC/DC buck converter for the auxiliary power module (APM) into one unit. The inverter housing is mounted to the transaxle to eliminate external phase cables and improve collision robustness. Due to the mounting location, additional considerations for vibration resistance were required, including rubber mounting bushings, elastic washer PCB mounting, and vibration simulations during the design of the signal interconnects.

The module and heat exchanger stack are shown in Fig. 3. The power module, manufactured in house by Toyota, is a phase leg "power card" format. The modules are resin molded with an integral heat exchanger allowing DSC. In total, seven phase leg modules, including their individual heat exchangers, are stacked to form the two VSIs and the DC/DC boost converter. The major benefit of the card format is simplified scalability of the inverter for different powertrain applications through paralleling of module. Interestingly the fourth generation module reintroduces thermal grease between the IGBT and heat exchanger, which had previously been eliminated in the third generation power module design. The additional heat flux from more tightly integrating the power switches is mitigated through the increased surface area of the DSC.

Improved power density has been achieved through the tight integration of many inverter components. The DC-link capacitor assembly for the inverters was designed to be connected directly to the power modules, eliminating the need for an additional busbar. The required capacitance was reduced thanks to improved control of the DC/DC boost converter while further reducing volume with new thinner polypropylene (PP) films. Snubber circuits, commonly used to limit the surge voltage across the switches, were eliminated through reducing stray inductance in the capacitors, busbars, and power modules. The phase current sensors have been integrated into the AC output terminals, relying on a Hall effect sensors that have been integrated into an IC package, reducing part count and simplifying assembly. Further size reductions were achieved by combining all control and gate drive circuitry onto a single PCB. Fastener count was reduced by 67% by transitioning to welded joins while simultaneously reducing fastener diameters to save space and weight.

C. Nissan MY2012 LEAF

The Nissan LEAF was first introduced in 2010 with a 24 kWh battery pack as Nissan's first mass market BEV. The MY2010 LEAF inverter and EM designs were documented by Nissan in a technical paper [52]. ORNL has conducted a teardown of the MY2012 LEAF inverter in [53] and the National Renewable Energy Laboratory (NREL) has published a performance evaluation of the thermal systems in [54].

The Nissan LEAF inverter is a single VSI powering the vehicle's one EM. The inverter is situated directly on top of the motor, eliminating external phase cables. As the vehicle has only a single EM and no ICE, packaging size of the inverter did not appear to be a significant priority in the design, thus the power density is somewhat low.

To achieve the required 340 A rms continuous current rating, three IGBTs and diodes are paralleled internally per switch with two switches forming a phase leg power module. A separate power module is used for each phase. The power module has a unique layer stack up in which the IGBT is soldered to an electrically conducting copper base plate with an intermediate copper molybdenum alloy buffer plate. The buffer material reduces stress caused by the CTE mismatch between the semiconductor and the copper plate. The copper plate is then bolted to the cooling plate with an electrically insulating thermal interface material. The gate drive circuitry includes dV/dt feedback through an analog differentiator coupled to the IGBT collector. During turn off events, the feedback controls the gate drive discharge to limit the turn off speed, reducing surge voltage.

The overall inverter layout is shown in Fig. 4. The DC-link capacitor is a large planar structure with DC terminals for

This article has been accepted for publication in a future issue of this journal, but has not been fully edited. Content may change prior to final publication. Citation information: DOI 10.1109/TVT.2019.2897899, IEEE Transactions on Vehicular Technology

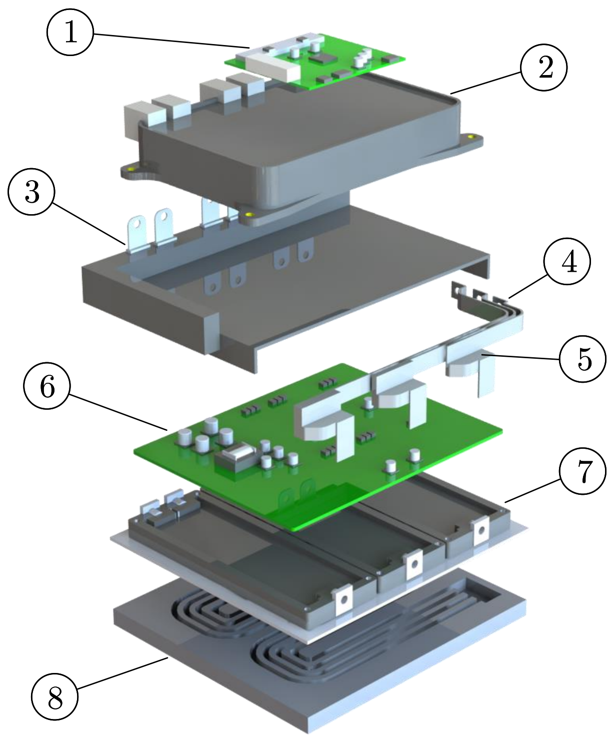

Fig. 4: Nissan LEAF inverter components [53]: 1) Control board 2) DC-link capacitor 3) DC-link busbar 4) Phase busbars 5) Current sensor 6) Gate driver board 7) IGBT power modules 8) Serpentine heat sink.

each of the three power modules and an integrated thermistor, manufactured by Panasonic. Three hall effect current sensors are integrated with the AC bus bar assembly. The gate driver board is located on top of the power modules while the control board is located above the DC-link capacitor. The cooling plate below the power modules has serpentine cooling channels for WEG coolant. The bottom cover is bolted with a gasket for sealing.

D. BMW MY2016 i3

The i3 is BMW's first mass produced zero emissions vehicle featuring either a 22 kW h or 33 kW h Lithium-ion battery and a 125 kW PM motor. ORNL has conducted a benchmarking assessment of the inverter and EM [55].

The inverter unit also contains an APM and a 3.7 kW battery charger and the overall unit weighs 19 kg. Again external phase cables have been eliminated by directly mounting the inverter on top of the EM. The power stage is an Infineon sixpack IGBT module which has a rated nominal collector current of 800A. The control board contains two DSPs as well as a complex programmable logic device (CPLD). The gate driver board also houses the three 700A LEM Hall effect current sensors for the phase outputs.

Mechanically, the inverter assembly is stacked with the DC-link capacitor on the bottom, followed by a cold plate on which the IGBT module is mounted. The gate driver board is mounted to the IGBT module and the control board is on top of the entire assembly. Since the control board also handles the charger and APM, it is much larger than the inverter stack and extends over much of the internal area.

E. Audi MY2016 A3 e-Tron

Volkswagen (VW) group recently released its new electrification project, named 'Roadmap E', for 2025 and its strategic approach seems to move towards more PHEVs and BEVs [56]. So far, the brands Audi, VW and Porsche have developed a dozen versions of their models with some degree of electrification. The VW group aims to massively expand its electrified portfolio across all brands and models by 2030.

Audi introduced in 2016 its new A3 e-Tron PHEV with a battery pack of 8.8 kWh allowing for an all-electric range of about 17 miles. In this parallel hybrid powertrain, a single 75 kW EM is combined with an ICE and the system delivers up to 152 kW and 350 N.m of torque.

In [57], the inverter module, manufactured by Bosch, is described. In order to maximize the packaging, the traction inverter and APM are integrated in the same enclosure and share a liquid cooled heat sink. The cooling plate is die cast as two aluminium pieces and then assembled via friction stir welding (FSW). The overall inverter module weight is estimated at 10 kg with a volume of about 8 L. Three IGBT half-bridge modules from Bosch are used in the traction inverter with voltage and current ratings of 600V and 300A respectively. The control board is composed of, amongst others, a processor, a microcontroller, and current sensor ICs, while the IGBT control board includes the gate drivers. The internal housing provides electromagnetic interference (EMI) shielding for the control board. Finally, a large DC-link metalized PP film capacitor is connected to the DC bus bar.

F. Tesla Model S

In 2012, Tesla introduced the Model S, a rear wheel drive full size luxury sedan with a range of up to 426 km with the 85 kWh battery pack. In 2014, Tesla announced an all wheel drive version of the Model S with an EM on both the front and rear axles. Relatively little engineering information is publicly available on the Tesla drive unit inverters, though several patents have been issued on the mechanical construction of the inverter. The rear drive unit from a 2015 Model S 70D, shown in Fig. 5, has been disassembled and the internal construction documented. The internal layout is shown in Fig. 6.

On the external cast aluminium housing, the coolant inlet and outlet ports are visible as well as a high voltage DC-link connector and a low voltage control connector. The cast housing is bolted to the gearbox housing in which an access port allows the inverter phase cables to be unbolted from the motor phase leads since they are entirely contained within the drive unit. The inverter consists of the control board which is on top of a stamped metal shield. Under the shield is a plastic cover which retains the silicone gel potting compound that encapsulates the gate driver board. Bus bars are layered beneath the gate driver board followed by the transistors and the DC-link capacitor which is at the bottom of the enclosure furthest from the gearbox. Current sensing is providing by two

This article has been accepted for publication in a future issue of this journal, but has not been fully edited. Content may change prior to final publication. Citation information: DOI 10.1109/TVT.2019.2897899, IEEE Transactions on Vehicular Technology

Fig. 5: Tesla Model S dual motor rear drive unit inverter.

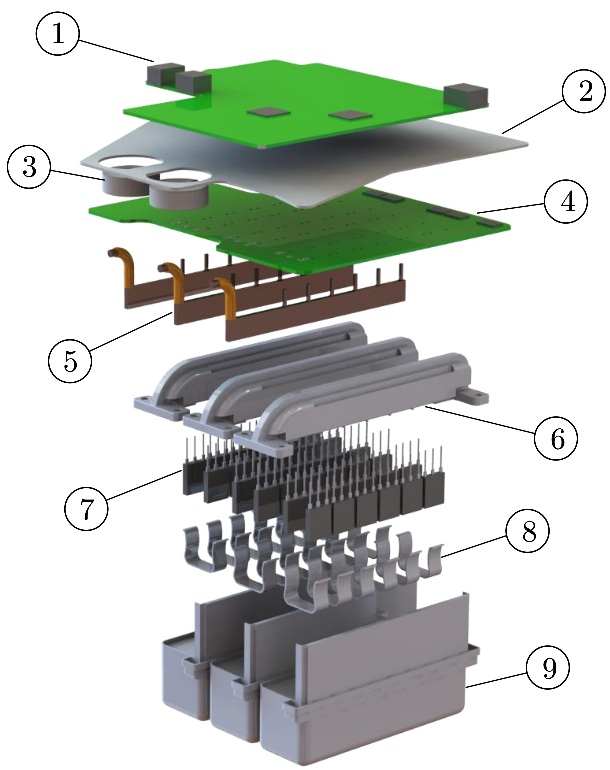

Fig. 6: Tesla Model S inverter components 1) Control board 2) Aluminium shield 3) Phase current sensor ferrite ring 4) Gate driver board 5) Phase busbars 6) Heat sinks 7) TO-247 package IGBTs 8) IGBT clips 9) DC-link capacitors.

Hall effect sensor ICs embedded in gapped soft ferromagnetic rings which surround two of the phase cables.

Unlike all other inverters surveyed, Tesla has opted for paralleling TO-247 discrete package IGBTs to achieve the required current ratings rather than using power modules. Six IGBTs are paralleled per switch for a total of 36 IGBTs. The IGBT leads are welded to the bus bars and the gate and emitter leads are additionally soldered to the gate drive board. Details of the process are contained in a Tesla patent on the welding and soldering of transistor leads [58]. A second patent describe the bus bar locating component which positions the DC positive and negative bus bars perpendicular to the transistors and the AC phase outputs parallel to the transistors [59].

Coolant from the inlet port is split into three distinct heat sinks which have six transistors affixed with clips to each side. The heat sinks are a two piece casting which is detailed in a third Tesla patent, including the internal fin geometry [60]. The DC-link capacitor is located below the transistor stage with a planar terminal connection to the DC bus bars, also described in a Tesla patent [61].

The weight and approximate volume of the inverter section of the drive unit was measured to be 5.8 kg and 6.4 L respectively.

IV. Future Trends

The DOE has identified several potential strategies towards achieving their 100 kW/L inverter target for 2025. Further integration of the inverter subcomponents is considered necessary, requiring advanced packaging capable of electrical and thermal isolation, while enabling significantly higher switching frequencies and power density. These tightly integrated components will require advanced thermal management systems and materials [5]. Several industry and research trends have also been identified in the areas of component packaging, gate driver design, system integration, and manufacturing techniques. Replacing silicon (Si) power semiconductors with wide bandgap (WBG) devices also brings significant opportunities to overcome the challenges associated with designing the next generation of traction inverters [63].

A. Topologies

It is expected the majority of automotive traction inverters will remain conventional two level VSIs. Multiphase two level inverters have been applied where high torque is a requirement, such as in buses and other heavy equipment. TM4 has developed six and nine phase inverters and accompanying PM machines for these applications [64]. As DC-link voltages increase, multilevel inverters become more attractive, however the cost of additional switching devices may make them impractical for consumer automotive applications. Research examples of multilevel traction inverters for heavy equipment have been developed [65, 66]. Switched reluctance motors (SRMs) have also received significant attention as a potential rare-earth material free traction machine. The conventional SRM is driven with an asymmetric bridge converter topology, which while distinct from a two level VSI, has similar requirements for the inverter components. SRM drives have also been commercially applied for traction purposes in heavy equipment [67].

B. WBG devices

The application of WBG semiconductors for power electronics including automotive traction inverters has been an area of significant research attention and the DOE has invested

This article has been accepted for publication in a future issue of this journal, but has not been fully edited. Content may change prior to final publication. Citation information: DOI 10.1109/TVT.2019.2897899, IEEE Transactions on Vehicular Technology

TABLE I: Inverter power density and specific power in recent EVs

Model	Components	Total Power Rating† (kVA)	Power Density (kVA/L)	Specific Power (kVA/kg)
Chevy Volt PHEV (2014) [46]	Dual inverter	180	17.3	21.7
Cadillac CT6 PHEV (2016) [48]	Dual inverter	215	22.6	16.0
Toyota Prius HEV (2016) [51]	Dual inverter, boost converter and APM	162	23.7	13.6
Nissan LEAF BEV (2012) [52]	Single inverter	80[a]	7.1	4.7
BMW i3 BEV (2016) [55]	Single inverter, charger and APM	125[a]	—[c]	6.6
Audi A3 e-Tron PHEV (2016) [57]	Single inverter and APM	75[a]	9.4	7.4
Tesla Model S 70D BEV (2015)	Single inverter	193[a,b]	30.1	33.3

† Total power rating is typically reported for only the inverter(s) while the mass and volume is reported for all components contained in the inverter housing, resulting in lower than actual estimates of power density and specific power. All values are peak output powers.
[a] Values are reported motor power in kW. Inverter kVA rating is likely slightly higher, resulting in lower than actual estimates of power density and specific power.
[b] Motor power as previously reported by Tesla [62]
[c] Volume not reported

heavily in their commercialization through the Advanced Research Projects Agency-Energy (ARPA-E) [68]. In fact, the aggressive 2025 power density targets are reliant on replacing traditional Si power transistors with WBG devices [5]. This is due to the fact that WBG devices have demonstrated numerous advantages over Si IGBTs including higher temperature operation, higher breakdown voltages, and higher switching frequencies while reducing both losses and chip size. Currently Silicon Carbide (SiC) and Gallium Nitride (GaN) are the most promising WBG materials due to their characteristics and commercialization progress [69]. SiC in particular has been an attractive candidate for traction inverters due to its superior high temperature operation which may enable system cost reductions through the unification of the inverter, EM, and even ICE liquid cooling loops [70].

The maximum DC-link voltage for BEVs is currently around $400\,\mathrm{V}$ however further increases are expected. Porsche and Fisker have both announced $800\,\mathrm{V}$ architectures with the goal of enabling faster charging rates [71, 72]. While Si devices are capable of $800\,\mathrm{V}$ operation, increased switching losses tend to reduce the efficiency making WBG devices an attractive solution for the traction inverter. In 2016, Toyota demonstrated a prototype SiC inverter for the Prius which was reported to achieve a 5% increase in fuel efficiency [73]. Mitsubishi Electric has also developed a prototype SiC traction inverter with a reported power density of 86 kVA/L [74].

Numerous research examples of WBG device based traction inverters have been reported in [75–78] and reviews on the status and applications of WBG devices to EVs have been conducted in [79–82]. While WBG devices offer many benefits over existing Si devices, the cost premium has been the primary barrier to adoption by automotive manufacturers. This cost is expected to continue to decline as manufacturing techniques improve and the market expands [83, 84]. As an intermediate step towards full WBG utilization, some semiconductor manufacturers have introduced hybrid devices which consist of a Si IGBT and SiC diode in one package. The SiC diode has negligible reverse recovery loss compared to an Si diode which is shown to reduce the total loss by 30-40% [85, 86]. Recently, it has been revealed that the Tesla Model 3 traction inverter is fully SiC MOSFET based with devices from STMicroelectronics [87].

C. Component packaging

Multiple approaches can be undertaken to improve the packaging of switching devices, resulting in superior thermal and electrical performance while reducing weight and size. Mitsubishi Electric launched a new IGBT module featuring a unified single layer insulated metal baseplate (IMB), providing both good insulation voltage and high thermal conductivity [88]. Conventionally, ceramic substrates are used for their low thermal resistance in combination with aluminum nitride substrates that provide the electrical insulation. By using the IMB technique, the single layer allows elimination of the bond wires between the substrates and the effective area for chip mounting can be increased by a reported 23%. The heat dissipation is also enhanced thanks to a reported 65% thermal resistance reduction.

Reliability improvements can also be realized through improved packaging and advanced thermal design. This has been achieved through innovations in the die attach process, enhanced interconnections, and cooling methods such as DSC. Manufacturers have begun to move away from bond wires and soldered connections as they show limitations under high current and high temperature operation [89, 90]. Semikron has developed their line of SKiM modules which use diffusion sinter connections to replace the thermal interface material, solder layers, and bond wires [91]. As a result, high reliability and extended lifetime are achieved under cyclic thermal stresses. Thermal management is also improved along with the power density by extending the heat dissipation area of the module. This is achieved with the DSC method that removes heat from both the top and bottom sides of the module, which can reduce the footprint up to 45% compared to the conventional singled-sided cooling technology [92]. In combination with DSC, bond wires for the top side of the chip can be replaced by planar interconnections [93]. By doing so, the thermal resistance as well as the stray inductance

This article has been accepted for publication in a future issue of this journal, but has not been fully edited. Content may change prior to final publication. Citation information: DOI 10.1109/TVT.2019.2897899, IEEE Transactions on Vehicular Technology

and parasitic resistance are reduced by 30%, 15%, and 75% respectively. Hence, the reliability and thermal capability of the system are increased along with the power density. The DSC technique has been implemented in production inverters by GM with Hitachi and Delphi Technologies modules, as well as by Toyota [57, 94, 95].

Besides the power semiconductors, the DC-link capacitors are also under the spotlight as they are typically the heaviest and most voluminous components in a traction inverter. To design their highly power dense inverter, Delphi Technologies and General Electric developed a novel polyyetherimide (PEI) capacitor dielectric film that can operate at higher temperatures [4]. Besides improvement of the capacitor technology itself, better integration of the capacitor with the DC side bus bar also enables some power density and efficiency improvements [96–98]. Indeed, by minimizing the series inductance in the DC side, the voltage overshoot across the switches can be reduced. Hence, the IGBT modules do not need to be as over designed to ensure a voltage safety margin and the inverter power density can be increased.

D. Thermal management

In addition to improvements in the device package, significant research has taken place investigating methods for removing heat from the devices. As device power density increases, it becomes more challenging to extract heat with a conventional liquid cold plate design. As a further improvement to the DSC design, direct cooling has been demonstrated in the Cadillac CT6 inverter in which the module package is fully immersed in the coolant, rather than bolted to a cold plate. Passive 2-phase immersion cooling has been successfully applied to large scale traction inverters for locomotives and mining equipment [99] for some time and may see future applications in automotive. Jet impingement and spray cooling have also received significant research attention [100], along with microchannel heatsinks and heatpipes.

E. Gate driver design

By pushing the performance of IGBT power semiconductors, gate drivers need to be more thoroughly designed and conventional passive circuits show limitations [31]. Indeed, gate drivers are usually designed based on the worst case scenario which limits the switching di/dt to prevent excessive surge voltage, increasing the switching losses. There is a trend to move towards smarter gate drivers that adapt the turn-on and turn-off slopes of the IGBT based on the operating conditions [101]. Active gate drive techniques enable more control of the switching behavior allowing the switching losses, surge voltage, and EMI emissions to be minimized [102]. For example, Ford developed a dynamic gate driver circuit that reduces the turn-off switching losses by up to 30% while ensuring low cost and similar surge voltage to a conventional gate driver [103]. Toyota developed a gate driver combining a two-stage gate voltage control with an additional feedback circuit [104]. This method achieves a good trade-off between surge voltage and switching losses. TM4 has commercialized their closed-loop gate drive technology which limits both the surge voltage and freewheeling diode recovery current [105]. Smart gate drivers also aim to integrate more protection and monitoring options, such as current and temperature sensing techniques, which can improve the reliability of the device and the inverter [106, 107]. Hitachi has also designed its own gate drivers for its highly power dense traction inverter [94, 108]. The gate driver IC features protection functions to detect excessive temperatures, over-current and under-voltage events. The Nissan LEAF inverter, described in section III-C, employs an active gate drive technique which uses dV/dt feedback from an analog differentiator in order to control the turn off speed, reducing surge voltage and switching losses. The circuit is shown in Fig. 7.

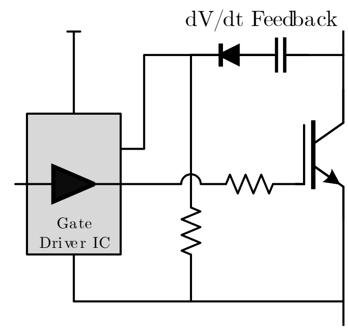

Fig. 7: dV/dt feedback active gate drive circuit used in the Nissan LEAF inverter [52].

Besides the need for IGBT gate driver improvements, WBG devices raise new challenges due to their high current densities, fast switching capabilities, and high temperature operation [109–112]. This impacts the driver ICs as they will also need to operate at higher temperatures and ensure higher voltage isolation barriers. Moreover, the fast switching behavior emphasizes the effects of the parasitics responsible for voltage overshoot and ringing. Integration of the driver IC with the power module is a suitable solution to limit the stray inductance as the distance between the gate and the chip is reduced. In [113], Navitas developed the first integrated half-bridge GaN power IC for 650 V that includes protection functions and sensing circuits.

F. System integration

Tighter integration of the traction inverter and EM has been a clear trend in production EVs. The majority of the production inverters surveyed in this paper have eliminated external phase cabling by packaging the inverter in direct proximity to the EM. This reduces both assembly and material cost while increasing reliability. Containing the phase cables within a common motor and inverter housing can also reduce radiated EMI emissions caused by the inverter.

Highly integrated inverters have been proposed in which the inverter electronics are mounted axially with the EM allowing a direct connection of the motor windings to the inverter phase terminals. This technique is not unprecedented; manufacturers have integrated rectifying diodes into the housings of automotive alternators for decades [114]. Multiphase machines are an excellent candidate for a highly integrated inverter as the lower

This article has been accepted for publication in a future issue of this journal, but has not been fully edited. Content may change prior to final publication. Citation information: DOI 10.1109/TVT.2019.2897899, IEEE Transactions on Vehicular Technology

phase currents allow the use of smaller switching devices which can be more easily arranged in a circular format while mitigating the need for additional phase cables. A prototype nine phase drivetrain including a PM machine, gearbox and integrated inverter has been developed to demonstrate the concept [115]. The integrated inverter is reported to achieve a power density of 35 kW/L with the entire system capable of a peak mechanical output power of 60 kW [116].

To further increase the level of integration between the EM and inverter, the concept of an integrated modular motor drive (IMMD) has been proposed [117]. The modularization of the machine into concentrated winding pole pieces each with integrated drive electronics allows a further reduction in the total drive volume and enables simultaneous optimization of the machine and inverter characteristics. WBG switching devices are an attractive candidate for IMMD designs as they are capable of the high temperature operation required given the proximity to the EM while also allowing a reduction in the DC-link capacitor sizing through increased switching frequency and interleaving techniques [118].

Manufacturers have already begun integration of the inverter with the other power electronics modules in the vehicle. This reduces weight and volume as a common housing can be used while potentially allowing sharing of the DC-link capacitor and thermal management systems. For the Chevrolet Volt and Cadillac CT6, GM integrates the dual inverters into the same enclosure and Audi A3 e-Tron combines the single inverter with the APM. The Prius dual inverter module contains the APM in addition to the high power DC/DC boost converter while the BMW i3 inverter integrates both the APM and the 3.7 kW on-board charger. Beyond simply physically integrating the power electronics modules into a single enclosure, there is an interest in integrated topologies that seek to reduce costs by reusing existing components and devices to achieve a new mode of functionality. In particular, integrated battery charger topologies have been proposed which use existing switching devices from the inverter and in some cases the motor winding leakage inductance to achieve battery charging functionality, eliminating the need for a dedicated on-board charger [119]. The concept has been implemented in a production vehicle in the Renault Zoe which is capable of charging at up to 43 kW with an integrated topology [120, 121].

G. Manufacturing techniques

Mass manufacturing of complex inverter assemblies is a challenging task due to the high number of distinct parts and stringent requirements for reliability and cost. In particular the liquid cooling system often has unique geometries and tight tolerances to optimize coolant flow, maintain a consistent thermal resistance and ensure there is no coolant leakage which could cause catastrophic failure of the inverter. In the current generation Chevrolet Volt and Audi e-Tron inverters, FSW techniques have been applied in the manufacturing process to ensure leak free joins of liquid cooling components without requiring gaskets and fasteners [122]. Heat is generated via friction with a non-consumable rotating tool against the faces of the parts to be joined. This effectively mixes the metals as the tool moves along the join resulting in a high quality weld with minimal distortion. Delphi Technologies has claimed a 45% reduction in footprint and a 50% shorter process time through their FSW manufacturing method for a liquid cooled heat exchanger which is integrated into the inverter housing [46].

Due to recent advances in manufacturing techniques, composite materials have seen a resurgence of interest for automotive applications which seek to improve vehicle efficiency and range through lightweighting. Composites can be up to 35% lighter than aluminium and 60% lighter than steel, reducing vehicle mass by up to 10% [123]. Several manufacturers have already adopted composite structural components including BMW which uses carbon fiber reinforced plastic extensively in the production of the i3 [124]. This trend may extend to housings and enclosures for vehicle components, including the traction inverter. Carbon fiber reinforced composite enclosures have already been marketed for aerospace applications and with continued cost reduction will become increasingly viable for automotive applications. In addition to the weight savings relative to metal enclosures, they are claimed to have superior EMI performance as the composite material can absorb the radiated emissions rather than reflecting it back to the source [125].

V. Conclusions

Traction inverters are a critical application of modern power electronics in developing more efficient, environmentally friendly automobiles. Detailed analysis of several production traction inverter designs is presented based on publications and reverse engineering efforts, including designs from recent model year GM, Toyota, Nissan, BMW, Audi, and Tesla vehicles. Based on the surveyed production inverters and ongoing industry and academic research, future trends in traction inverter design are identified. WBG devices have been of interest for automotive power electronics systems for some time and are just now beginning to see adoption with the industry's first fully SiC traction inverter in the Tesla Model 3. It is likely other manufacturers will follow suit and WBG device costs will further decline as demand increases, resulting in a new generation of WBG based traction inverters with improved efficiency and power density.

Power semiconductor packaging and thermal management has played a large role in improving inverter reliability and power density. Several manufacturers have now moved to DSC IGBT modules to facilitate lower thermal resistances and increased cooling surface area. Gate driver design has also become critical to increase efficiency, with active gate drive designs reporting up to a 30% reduction in IGBT turn off losses. Fully integrated active gate drive ICs are likely to become widely available, reducing the cost and complexity issues that are currently a challenge for active gate drive techniques.

At the system level, tighter integration of the inverter with both the EM and other power electronics modules in the vehicle will result in cost and weight savings. Several manufacturers have already integrated the APM or on-board charger into the inverter housing allowing a shared DC-link capacitor and thermal management system. Direct integration of the inverter electronics into the EM housing may present opportunities for further power density improvements as well as the implementation of multiphase machines in certain applications. Challenges with vibration robustness and high temperature operation need to be addressed as manufacturers proceed with further integration of the inverter and EM.

Traction inverter design is a challenging and inherently interdisciplinary engineering problem with many competing objectives. It is clear from industry examples that there are multiple valid approaches even with a single standard circuit topology. As more manufacturers introduce EVs with mass market appeal, further innovative solutions will be required to meet the widely varying demands of various automotive applications.

Acknowledgement

This research was undertaken, in part, thanks to funding from the Canada Excellence Research Chairs Program.

References

[1] B. Bilgin, P. Magne, P. Malysz, Y. Yang, V. Pantelic, M. Preindl, A. Korobkine, W. Jiang, M. Lawford, and A. Emadi, "Making the case for electrified transportation," *IEEE Transactions on Transportation Electrification*, vol. 1, no. 7, pp. 4–17, June 2015.

[2] A. Emadi, *Advanced Electric Drive Vehicles*. CRC Press Taylor and Francis Group, Oct. 2014.

[3] "U.S. DRIVE Electrical and Electronics Technical Team Roadmap," U.S. Department of Energy, June 2013.

[4] S. A. Rogers, "Annual progress report for the advanced power electronics and electric motors program," U.S. Department of Energy, Tech. Rep. DOE/EE-1040, Dec. 2013.

[5] "U.S. DRIVE Electrical and Electronics Technical Team Roadmap," U.S. Department of Energy, Oct. 2017.

[6] K. Rajashekara, "Present status and future trends in electric vehicle propulsion technologies," *IEEE Journal of Emerging and Selected Topics in Power Electronics*, vol. 1, no. 1, pp. 3–10, 2013.

[7] H. Ye, Y. Yang, and A. Emadi, "Traction inverters in hybrid electric vehicles," in *2012 IEEE Transportation Electrification Conference and Expo (ITEC)*, June 2012, pp. 1–6.

[8] M. H. Rashid, *Power electronics handbook*. Butterworth-Heinemann, 2017.

[9] L. Concari, D. Barater, C. Concari, A. Toscani, G. Buticchi, and M. Liserre, "H8 architecture for reduced common-mode voltage three-phase pv converters with silicon and sic power switches," in *IECON 2017 - 43rd Annual Conference of the IEEE Industrial Electronics Society*, Oct. 2017, pp. 4227–4232.

[10] F. Hasanzad, H. Rastegar, and M. Pichan, "Performance analysis of reduced common-mode voltage space vector modulation techniques for three-phase four-leg voltage-source inverter," in *2018 9th Annual Power Electronics, Drives Systems and Technologies Conference (PEDSTC)*, Feb. 2018, pp. 65–70.

[11] T. Hadden, J. W. Jiang, B. Bilgin, Y. Yang, A. Sathyan, H. Dadkhah, and A. Emadi, "A review of shaft voltages and bearing currents in EV and HEV motors," in *IECON 2016 - 42nd Annual Conference of the IEEE Industrial Electronics Society*, Oct. 2016, pp. 1578–1583.

[12] Z. Wu and G. Su, "High-performance permanent magnet machine drive for electric vehicle applications using a current source inverter," in *2008 34th Annual Conference of IEEE Industrial Electronics*, Nov. 2008, pp. 2812–2817.

[13] E. P. Wiechmann, P. Aqueveque, R. Burgos, and J. Rodríguez, "On the efficiency of voltage source and current source inverters for high-power drives," *IEEE Transactions on Industrial Electronics*, vol. 55, no. 4, pp. 1771–1782, 2008.

[14] F. Z. Peng, "Z-source inverter," *IEEE Transactions on industry applications*, vol. 39, no. 2, pp. 504–510, 2003.

[15] F. Z. Peng, A. Joseph, J. Wang, M. Shen, L. Chen, Z. Pan, E. Ortiz-Rivera, and Y. Huang, "Z-source inverter for motor drives," *IEEE Transactions on Power Electronics*, vol. 20, no. 4, pp. 857–863, July 2005.

[16] F. Z. Peng, M. Shen, and K. Holland, "Application of Z-source inverter for traction drive of fuel cell—battery hybrid electric vehicles," *IEEE Transactions on Power Electronics*, vol. 22, no. 3, pp. 1054–1061, 2007.

[17] M. Shen, A. Joseph, J. Wang, F. Z. Peng, and D. J. Adams, "Comparison of traditional inverters and Z-source inverter for fuel cell vehicles," *IEEE Transactions on Power Electronics*, vol. 22, no. 4, pp. 1453–1463, 2007.

[18] J. Rodriguez, J.-S. Lai, and F. Z. Peng, "Multilevel inverters: a survey of topologies, controls, and applications," *IEEE Transactions on Industrial Electronics*, vol. 49, no. 4, pp. 724–738, Aug. 2002.

[19] J. Rodriguez, S. Bernet, P. K. Steimer, and I. E. Lizama, "A survey on neutral-point-clamped inverters," *IEEE Transactions on Industrial Electronics*, vol. 57, no. 7, pp. 2219–2230, July 2010.

[20] M. Schweizer and J. W. Kolar, "Design and implementation of a highly efficient three-level T-type converter for low-voltage applications," *IEEE Transactions on Power Electronics*, vol. 28, no. 2, pp. 899–907, 2013.

[21] R. Teichmann and S. Bernet, "A comparison of three-level converters versus two-level converters for low-voltage drives, traction, and utility applications," *IEEE Transactions on Industry Applications*, vol. 41, no. 3, pp. 855–865, 2005.

[22] M. Schweizer, T. Friedli, and J. W. Kolar, "Comparative evaluation of advanced three-phase three-level inverter/converter topologies against two-level systems," *IEEE Transactions on industrial electronics*, vol. 60, no. 12, pp. 5515–5527, 2013.

[23] D. G. Holmes and T. A. Lipo, *Pulse width modulation for power converters: principles and practice*. John Wiley & Sons, 2003.

[24] A. Mehrizi-Sani and S. Filizadeh, "An optimized space vector modulation sequence for improved harmonic performance," *IEEE Transactions on Industrial Electronics*, vol. 56, no. 8, pp. 2894–2903, 2009.

[25] H. W. Van Der Broeck, H.-C. Skudelny, and G. V. Stanke, "Analysis and realization of a pulsewidth modulator based on voltage space vectors," *IEEE transactions on industry applications*, vol. 24, no. 1, pp. 142–150, 1988.

[26] A. Cataliotti, F. Genduso, A. Raciti, and G. R. Galluzzo, "Generalized PWM-VSI control algorithm based on a universal duty-cycle expression: Theoretical analysis, simulation results, and experimental validations," *IEEE Transactions on Industrial Electronics*, vol. 54, no. 3, pp. 1569–1580, 2007.

[27] S. Jurkovic, K. Rahman, B. Bae, N. Patel, and P. Savagian, "Next generation Chevy Volt electric machines; design, optimization and control for performance and rare-earth mitigation," in *2015 IEEE Energy Conversion Congress and Exposition (ECCE)*, Sept. 2015, pp. 5219–5226.

[28] F. Momen, K. Rahman, Y. Son, and P. Savagian, "Electrical propulsion system design of Chevrolet Bolt battery electric vehicle," in *2016 IEEE Energy Conversion Congress and Exposition (ECCE)*, Sept. 2016, pp. 1–8.

[29] J. Holtz, W. Lotzkat, and A. Khambadkone, "On continuous control of pwm inverters in the overmodulation range including the six-step mode," in *Proceedings of the 1992 International Conference on Industrial Electronics, Control, Instrumentation, and Automation*, Nov. 1992, pp. 307–312 vol.1.

[30] D. H. Ward, C. Iqbal, A. Carlos Volke, and M. Hornkamp,

Fundamentals of Semiconductors for Hybrid-Electric Powertrain. Infineon Technologies North America Corp, 2013.

[31] Y. Lobsiger and J. W. Kolar, "Closed-loop di/ dt and dv/dt IGBT gate driver," *IEEE Transactions on Power Electronics*, vol. 30, no. 6, pp. 3402–3417, 2015.

[32] L. Diao, J. Tang, P. C. Loh, S. Yin, L. Wang, and Z. Liu, "An efficient DSP–FPGA-based implementation of hybrid PWM for electric rail traction induction motor control," *IEEE Transactions on Power Electronics*, vol. 33, no. 4, pp. 3276–3288, Apr. 2018.

[33] M. Lakka, E. Koutroulis, and A. Dollas, "Development of an FPGA-based SPWM generator for high switching frequency DC/AC inverters," *IEEE Transactions on Power Electronics*, vol. 29, no. 1, pp. 356–365, 2014.

[34] X. Pei, W. Zhou, and Y. Kang, "Analysis and calculation of DC-link current and voltage ripples for three-phase inverter with unbalanced load," *IEEE Transactions on Power Electronics*, vol. 30, no. 10, pp. 5401–5412, 2015.

[35] J. Guo, J. Ye, and A. Emadi, "DC-link current and voltage ripple analysis considering antiparallel diode reverse recovery in voltage source inverters," *IEEE Transactions on Power Electronics*, vol. 33, no. 6, pp. 5171–5180, 2018.

[36] H. Wen, W. Xiao, X. Wen, and P. Armstrong, "Analysis and evaluation of DC-link capacitors for high-power-density electric vehicle drive systems," *IEEE Transactions on Vehicular Technology*, vol. 61, no. 7, pp. 2950–2964, 2012.

[37] M. A. Vogelsberger, T. Wiesinger, and H. Ertl, "Life-cycle monitoring and voltage-managing unit for DC-link electrolytic capacitors in pwm converters," *IEEE Transactions on Power Electronics*, vol. 26, no. 2, pp. 493–503, 2011.

[38] V. Smet, F. Forest, J. Huselstein, F. Richardeau, Z. Khatir, S. Lefebvre, and M. Berkani, "Ageing and failure modes of IGBT modules in high-temperature power cycling," *IEEE Transactions on Industrial Electronics*, vol. 58, no. 10, pp. 4931–4941, Oct. 2011.

[39] Y. Yamada, Y. Takaku, Y. Yagi, I. Nakagawa, T. Atsumi, M. Shirai, I. Ohnuma, and K. Ishida, "Reliability of wire-bonding and solder joint for high temperature operation of power semiconductor device," *Microelectronics Reliability*, vol. 47, no. 12, pp. 2147–2151, 2007.

[40] J. Ye, K. Yang, H. Ye, and A. Emadi, "A fast electro-thermal model of traction inverters for electrified vehicles," *IEEE Transactions on Power Electronics*, vol. 32, no. 5, pp. 3920–3934, 2017.

[41] K. Ma, A. S. Bahman, S. Beczkowski, and F. Blaabjerg, "Complete loss and thermal model of power semiconductors including device rating information," *IEEE Transactions on Power Electronics*, vol. 30, no. 5, pp. 2556–2569, 2015.

[42] A. S. Bahman, K. Ma, and F. Blaabjerg, "A lumped thermal model including thermal coupling and thermal boundary conditions for high-power IGBT modules," *IEEE Transactions on Power Electronics*, vol. 33, no. 3, pp. 2518–2530, 2018.

[43] Z. Luo, H. Ahn, and M. Nokali, "A thermal model for insulated gate bipolar transistor module," *IEEE Transactions on Power Electronics*, vol. 19, no. 4, pp. 902–907, 2004.

[44] E. Laloya, O. Lucia, H. Sarnago, and J. M. Burdio, "Heat management in power converters: From state of the art to future ultrahigh efficiency systems," *IEEE Transactions on Power Electronics*, vol. 31, no. 11, pp. 7896–7908, 2016.

[45] A. D. Callegaro, J. Guo, M. Eull, B. Danen, J. Gibson, M. Preindl, B. Bilgin, and A. Emadi, "Bus bar design for high-power inverters," *IEEE Transactions on Power Electronics*, vol. 33, no. 3, pp. 2354–2367, 2018.

[46] M. Anwar, M. Hayes, A. Tata, M. Teimorzadeh, and T. Achatz, "Power dense and robust traction power inverter for the second-generation chevrolet volt extended-range EV," *SAE International Journal of Alternative Powertrains*, vol. 4, no. 2015-01-1201, pp. 145–152, 2015.

[47] M. Anwar, S. M. N. Hasan, M. Teimor, M. Korich, and M. B. Hayes, "Development of a power dense and environmentally robust traction power inverter for the second-generatio chevrolet volt extended-range ev," in *2015 IEEE Energy Conversion Congress and Exposition (ECCE)*, Sept. 2015, pp. 6006–6013.

[48] M. Anwar, M. Teimor, P. Savagian, R. Saito, and T. Matsuo, "Compact and high power inverter for the cadillac ct6 rear wheel drive PHEV," in *2016 IEEE Energy Conversion Congress and Exposition (ECCE)*, Sept. 2016, pp. 1–7.

[49] A. Khan, T. Grewe, J. Liu, M. Anwar, A. Holmes, and R. Balsley, "The GM RWD PHEV propulsion system for the Cadillac CT6 luxury sedan," in *SAE 2016 World Congress and Exhibition*. SAE International, Apr. 2016.

[50] T. A. Burress, S. L. Campbell, C. L. Coomer, C. W. Ayers, A. A. Wereszczak, J. P. Cunningham, L. D. Marlino, L. E. Seiber, and H. T. Lin, "Evaluation of the 2010 Prius hybrid synergy drive system," Oak Ridge National Laboratory, Tech. Rep. ORNL/TM-2010/253, Jan. 2008.

[51] O. Kitazawa, T. Kikuchi, M. Nakashima, Y. Tomita, H. Kosugi, and T. Kaneko, "Development of power control unit for compact-class vehicle," *SAE International Journal of Alternative Powertrains*, vol. 5, pp. 278–285, 04 2016.

[52] Y. Sato, S. Ishikawa, T. Okubo, M. Abe, and K. Tamai, "Development of high response motor and inverter system for the Nissan LEAF electric vehicle," in *SAE 2011 World Congress & Exhibition*. SAE International, 04 2011.

[53] T. Burress. (2013) Benchmarking state-of-the-art technologies. Oak Ridge National Laboratory. [Online]. Available: http://energy.gov/sites/prod/files/2014/03/f13/ape006_burress_2013_o.pdf

[54] G. Moreno, K. Bennion, C. King, and S. Narumanchi, "Evaluation of performance and opportunities for improvements in automotive power electronics systems," in *2016 15th IEEE Intersociety Conference on Thermal and Thermomechanical Phenomena in Electronic Systems (ITherm)*, May 2016, pp. 185–192.

[55] M. Olszewski, "Oak ridge national laboratory annual progress report for the power electronics and electric machinery program," Oak Ridge National Laboratory (ORNL), Oak Ridge, TN, Tech. Rep., 2016.

[56] Roadmap E: full of energy! Volkswagen Group. [Online]. Available: https://www.volkswagenag.com/en/news/stories/2018/04/roadmap-e-full-of-energy.html

[57] R. Taylor, "Advanced strong hybrid and plug-in hybrid engineering evaluation and cost analysis," Munro and Associates Inc., Ricardo Strategic Consulting and ZMassociates Environmental Corp, Tech. Rep., Apr. 2017.

[58] R. J. Ramm, W. Liu, and C. Campbell, "Welding and soldering of transistor leads," U.S. Patent US14 557 381, 2014.

[59] R. J. Ramm, D. Sasaridis, C. Campbell, and W. Liu, "Busbar locating component," U.S. Patent US14 557 398, 2014.

[60] R. J. Ramm, W. Liu, and C. Campbell, "Heatsink with internal cavity for liquid cooling," U.S. Patent US14 286 670, 2014.

[61] R. J. Ramm, D. Sasaridis, C. Campbell, and W. Liu, "Planar capacitor terminals," U.S. Patent US14 557 256, 2014.

[62] E. Loveday. (2015) Tesla Modifies Horsepower Ratings For Dual Motor Model S. Inside EVs. [Online]. Available: https://insideevs.com/tesla-modifies-horsepower-ratings-dual-motor-model-s/

[63] K. Hamada, "Present status and future prospects for electronics in EVs/HEVs and expectations for wide bandgap semiconductor devices," in *Materials Science Forum*, vol. 600. Trans Tech Publ, 2009, pp. 889–893.

[64] (2018) TM4 SUMO product brochure. TM4. [Online]. Available: https://www.tm4.com/wp-content/uploads/2018/08/TM4-SUMO-Product-Brochure.pdf

[65] Z. Wang, M. H. Mahmud, M. H. Uddin, B. McPherson, B. Sparkman, Y. Zhao, H. A. Mantooth, and J. R. Fraley, "A compact 250 kW silicon carbide MOSFET based three-level traction inverter for heavy equipment applications," *2018 IEEE*

Transportation Electrification Conference and Expo (ITEC), pp. 1129–1134, 2018.

[66] S. Bhattacharya, D. Mascarella, G. Joos, J.-M. Cyr, and J. Xu, "A dual three-level T-NPC inverter for high-power traction applications," *IEEE Journal of Emerging and Selected Topics in Power Electronics*, vol. 4, no. 2, pp. 668–678, June 2016.

[67] B. Singh, "Novel and ruggedized power electronics for off-highway vehicles," *IEEE Electrification Magazine*, vol. 2, no. 2, pp. 31–41, June 2014.

[68] US Department of Energy, "Wide bandgap semiconductors for power electronics technology assessment," *Quadrennial Technology Review*, 2015.

[69] J. Millan, P. Godignon, X. Perpina, A. Perez-Tomas, and J. Rebollo, "A survey of wide bandgap power semiconductor devices," *IEEE Transactions on Power Electronics*, vol. 29, no. 5, pp. 2155–2163, May 2014.

[70] A. Antonopoulos, H. Bangtsson, M. Alakula, and S. Manias, "Introducing a silicon carbide inverter for hybrid electric vehicles," in *2008 IEEE Power Electronics Specialists Conference*. IEEE, June 2008, pp. 1321–1325.

[71] V. Reber, "E-power: New possibilities with 800-volt charging," *Porsche Engineering Magazine*, no. 1, pp. 10–15, 2016. [Online]. Available: https://www.porscheengineering.com/peg/en/about/magazine/

[72] (2017, Oct.) Fisker Inc. chooses Ricardo to support integration of state-of-the-art 800V electric powertrain. [Online]. Available: https://d1v9sz08rbysvx.cloudfront.net/ricardo/media/media/other%20download%20files/fisker-ricardo-release-final-draft.pdf

[73] T. Ogawa, A. Tanida, T. Yamakawa, and M. Okamura, "Verification of fuel efficiency improvement by application of highly effective silicon carbide power semiconductor to HV inverter," in *SAE 2016 World Congress and Exhibition*, Apr. 2016.

[74] S. Yano, Y. Nakayama, H. Kobayashi, S. Hiramatsu, M. Yoshida, K. Onda, K. Hayashi, and K. Yamazaki, "Development of compact power control unit for HEVs," in *2017 IEEE Energy Conversion Congress and Exposition (ECCE)*, Oct. 2017, pp. 584–588.

[75] M. Eull, M. Preindl, and A. Emadi, "Analysis and design of a high efficiency, high power density three-phase silicon carbide inverter," in *2016 IEEE Transportation Electrification Conference and Expo (ITEC)*. IEEE, June 2016, pp. 1–6.

[76] J. Colmenares, D. Peftitsis, J. Rabkowski, D.-P. Sadik, G. Tolstoy, and H.-P. Nee, "High-efficiency 312-kVA three-phase inverter using parallel connection of silicon carbide MOSFET power modules," *IEEE Transactions on Industry Applications*, vol. 51, no. 6, pp. 4664–4676, Nov. 2015.

[77] J. Zhu, H. Kim, H. Chen, R. Erickson, and D. Maksimović, "High efficiency sic traction inverter for electric vehicle applications," in *2018 IEEE Applied Power Electronics Conference and Exposition (APEC)*, Mar. 2018, pp. 1428–1433.

[78] J. Casady, K. Olejniczak, T. McNutt, D. Simco, B. Passmore, R. Shaw, D. Martin, A. Curbow, B. Hull, and J. Palmour, "88 kilowatt automotive inverter with new 900 volt silicon carbide MOSFET technology," Cree, Inc., Fayetteville, AR (United States), Tech. Rep. DOE-Cree-0006920, Oct. 2017.

[79] F. Shang, A. P. Arribas, and M. Krishnamurthy, "A comprehensive evaluation of SiC devices in traction applications," *2014 IEEE Transportation Electrification Conference and Expo (ITEC)*, pp. 1–5, 2014.

[80] A. Morya, M. Moosavi, M. C. Gardner, and H. A. Toliyat, "Applications of wide bandgap (WBG) devices in AC electric drives: A technology status review," *2017 IEEE International Electric Machines and Drives Conference, IEMDC 2017*, 2017.

[81] D. Han, S. Li, W. Lee, and B. Sarlioglu, "Adoption of wide bandgap technology in hybrid/electric vehicles-opportunities and challenges," in *2017 IEEE Transportation Electrification Conference and Expo (ITEC)*, vol. 3. IEEE, June 2017, pp. 561–566.

[82] H. Zhang, L. M. Tolbert, and B. Ozpineci, "Impact of SiC devices on hybrid electric and plug-in hybrid electric vehicles," *IEEE Transactions on Industry Applications*, vol. 47, no. 2, pp. 912–921, March 2011.

[83] S. Das, L. D. Marlino, and K. O. Armstrong, "Wide bandgap semiconductor opportunities in power electronics," Oak Ridge National Lab.(ORNL), Oak Ridge, TN (United States), Tech. Rep. ORNL/TM-2017/702, 2018.

[84] M. Su, C. Chen, S. Sharma, and J. Kikuchi, "Performance and cost considerations for sic-based hev traction inverter systems," in *2015 IEEE 3rd Workshop on Wide Bandgap Power Devices and Applications (WiPDA)*, Nov. 2015, pp. 347–350.

[85] B. Ozpineci, M. S. Chinthavali, L. M. Tolbert, A. S. Kashyap, and H. A. Mantooth, "A 55-kw three-phase inverter with Si IGBTs and SiC schottky diodes," *IEEE Transactions on Industry Applications*, vol. 45, no. 1, pp. 278–285, 2009.

[86] L. Amber and K. Haddad, "Hybrid si igbt-sic schottky diode modules for medium to high power applications," in *2017 IEEE Applied Power Electronics Conference and Exposition (APEC)*, Mar. 2017, pp. 3027–3032.

[87] (2018) Tesla model 3 inverter with SiC power module from ST Microelectronics. SYSTEMPlus Consulting. [Online]. Available: http://www.systemplus.fr/wp-content/uploads/2018/06/SP18413-STMicroelectronics-SiC-Module-Tesla-Model3-Inverter_flyer-1.pdf

[88] K. Ohara, H. Masumoto, T. Takahashi, . M. Matsumoto, and Y. Otsubo, "A new IGBT module with insulated metal baseplate (IMB) and 7th generation chips," in *Proceedings of PCIM Europe 2015; International Exhibition and Conference for Power Electronics, Intelligent Motion, Renewable Energy and Energy Management*, May 2015, pp. 1–4.

[89] Z. Liang, "Status and trend of automotive power packaging," in *2012 24th International Symposium on Power Semiconductor Devices and ICs*, June 2012, pp. 325–331.

[90] M. R. Atelge, "Power module packaging in automotive applications," Master's thesis, University of Waterloo, 2016.

[91] J. Steger, "A new generation of power modules with sinter-technology for the automotive industry," in *2011 1st International Electric Drives Production Conference*, 2011, pp. 60–62.

[92] T. Geinzer, A. Schwarz, and M. Gleich, "Innovations for IGBT based power modules in HEV drivetrain applications," in *PCIM Europe 2017; International Exhibition and Conference for Power Electronics, Intelligent Motion, Renewable Energy and Energy Management; Proceedings of*, Nuremberg, Germany, May 2017, pp. 1–3.

[93] Y. Wang, Y. Li, X. Dai, S. Zhu, S. Jones, and G. Liu, "Thermal design of a dual sided cooled power semiconductor module for hybrid and electric vehicles," in *2017 IEEE Applied Power Electronics Conference and Exposition (APEC)*, 2017, pp. 3068–3071.

[94] T. Kimura, R. Saitou, K. Kubo, K. Nakatsu, H. Ishikawa, and K. Sasaki, "High-power-density inverter technology for hybrid and electric vehicle applications," *Hitachi Review*, vol. 63, no. 2, pp. 96–102, 2014.

[95] T. Tokuyama, K. Nakatsu, A. Nishihara, K. Sasaki, and R. Saito, "A novel direct water and double-sided cooled power module for HEV/EV inverter," *2014 International Conference on Electronics Packaging, ICEP 2014*, pp. 6–9, 2014.

[96] M. Brubaker, D. El Hage, T. Hosking, E. Sawyer, and W. T. Franke, "Integrated DC link capacitor/bus enables a 20% increase in inverter efficiency," *PCIM Europe Conference Proceedings*, no. May, pp. 501–508, 2014.

[97] E. Sawyer, M. Brubaker, and T. Hosking, "Understanding the contribution of switch input connection geometry to overall DC link inductance," in *2015 17th European Conference on Power Electronics and Applications (EPE'15 ECCE-Europe)*, 2015, pp. 1–8.

This article has been accepted for publication in a future issue of this journal, but has not been fully edited. Content may change prior to final publication. Citation information: DOI 10.1109/TVT.2019.2897899, IEEE Transactions on Vehicular Technology

[98] M. A. Brubaker, T. A. Hosking, T. Reiter, L. D. Marlino, and M. S. Chinthavali, "Optimized DC link for next generation power modules," in *PCIM Europe 2016; International Exhibition and Conference for Power Electronics, Intelligent Motion, Renewable Energy and Energy Management*, 2016, pp. 1–9.

[99] C. M. Barnes and P. E. Tuma, "Practical considerations relating to immersion cooling of power electronics in traction systems," *IEEE Transactions on Power Electronics*, vol. 25, no. 9, pp. 2478–2485, Sept. 2010.

[100] J. Broughton, V. Smet, R. R. Tummala, and Y. K. Joshi, "Review of thermal packaging technologies for automotive power electronics for traction purposes," *Journal of Electronic Packaging*, vol. 140, no. 4, p. 040801, 2018.

[101] J. Chen and W. Ng, "Design trends in smart gate driver ICs for power MOSFETs and IGBTs," in *2017 IEEE 12th International Conference on ASIC (ASICON)*, 2017, pp. 112–115.

[102] N. Idir, R. Bausiere, and J. J. Franchaud, "Active gate voltage control of turn-on di/dt and turn-off dv/dt in insulated gate transistors," *IEEE Transactions on Power Electronics*, vol. 21, no. 4, pp. 849–855, 2006.

[103] Y. Zhou, L. Chen, S. Yang, F. Xu, and A. Khorshed, "A low cost gate driver with dynamic turn-off transient control for HEV/EV traction inverter application," *Conference Proceedings - IEEE Applied Power Electronics Conference and Exposition - APEC*, pp. 3200–3204, 2017.

[104] Y. Osanai, M. Wasekura, H. Yamawaki, and Y. Shindo, "IGBT gate control methods to reduce electrical power losses of hybrid vehicles," in *SAE 2016 World Congress and Exhibition*. SAE International, Apr. 2016.

[105] J.-M. Cyr, "Optimisation of IGBTs during the commutation process," TM4, Tech. Rep., 2015.

[106] H. Niu and R. D. Lorenz, "Sensing IGBT junction temperature using gate drive output transient properties," in *2015 IEEE Applied Power Electronics Conference and Exposition (APEC)*, 2015, pp. 2492–2499.

[107] D. Bortis, J. Biela, and J. W. Kolar, "Active gate control for current balancing of parallel-connected IGBT modules in solid-state modulators," *IEEE Transactions on Plasma Science*, vol. 36, no. 5, pp. 2632–2637, 2008.

[108] N. Sakurai and K. Yahata, "Gate driver integrated circuit for high-current and high-speed insulated-gate bipolar transistors used in hybrid electric vehicle and electric vehicle inverters," in *2017 IEEE 3rd International Future Energy Electronics Conference and ECCE Asia (IFEEC 2017 - ECCE Asia)*, 2017, pp. 947–952.

[109] B. Wang, M. Riva, J. D. Bakos, and A. Monti, "Integrated circuit implementation for a GaN HFET driver circuit," *IEEE Transactions on Industry Applications*, vol. 46, no. 5, pp. 2056–2067, 2010.

[110] Z. Wang, X. Shi, Y. Xue, L. M. Tolbert, F. Wang, and B. J. Blalock, "Design and performance evaluation of over current protection schemes for silicon carbide (SiC) power MOSFETs," *IEEE Transactions on Industrial Electronics*, vol. 61, no. 10, pp. 5570–5581, 2014.

[111] A. Rujas, V. López-Martín, L. Mir, and T. Nieva, "Gate driver for high power SiC modules. design considerations, development and experimental validation." *IET Power Electronics*, 2017.

[112] G. S. Inc., "Application brief:how to drive GaN enhancement mode HEMT," GaN Systems Inc., Tech. Rep. GN001, Apr. 2016.

[113] N. Fichtenbaum, M. Giandalia, S. Sharma, and J. Zhang, "Half-bridge gan power ICs: Performance and application," *IEEE Power Electronics Magazine*, vol. 4, no. 3, pp. 33–40, 2017.

[114] T. M. Jahns, "The past, present, and future of power electronics integration technology in motor drives," *CPSS Transactions on Power Electronics and Applications*, vol. 2, no. 3, pp. 197–216, Sept. 2017.

[115] Y. Burkhardt, A. Spagnolo, P. Lucas, M. Zavesky, and P. Brockerhoff, "Design and analysis of a highly integrated 9-phase drivetrain for EV applications," in *2014 International Conference on Electrical Machines (ICEM)*. IEEE, Sept. 2014, pp. 450–456.

[116] P. Brockerhoff, W. Schon, P. Blaha, P. Vaclavek, and Y. Burkhardt, "Disc inverter in highly integrated 9-phase drivetrain for E-mobility," in *2015 17th European Conference on Power Electronics and Applications (EPE'15 ECCE-Europe)*. IEEE, Sept. 2015, pp. 1–9.

[117] N. R. Brown, T. M. Jahns, and R. D. Lorenz, "Power converter design for an integrated modular motor drive," in *2007 IEEE Industry Applications Annual Meeting*. IEEE, Sept. 2007, pp. 1322–1328.

[118] J. Wang, Y. Li, and Y. Han, "Integrated modular motor drive design with GaN power FETs," *IEEE Transactions on Industry Applications*, vol. 51, no. 4, pp. 3198–3207, 2015.

[119] N. Sakr, D. Sadarnac, and A. Gascher, "A review of onboard integrated chargers for electric vehicles," in *2014 16th European Conference on Power Electronics and Applications*. IEEE, Aug. 2014, pp. 1–10.

[120] I. Subotic, N. Bodo, and E. Levi, "An EV drive-train with integrated fast charging capability," *IEEE Transactions on Power Electronics*, vol. 31, no. 2, pp. 1461–1471, Feb. 2016.

[121] S. Loudot, B. Briane, O. Ploix, and A. Villeneuve, "Fast charging device for an electric vehicle," U.S. Patent US12 919 396, 2010.

[122] A. Steier and A. Munday, "Advanced strong hybrid and plug-in hybrid engineering evaluation and cost analysis," California Air Resources Board, Tech. Rep., 2017.

[123] S. Das, "Life cycle assessment of carbon fiber-reinforced polymer composites," *The International Journal of Life Cycle Assessment*, vol. 16, no. 3, pp. 268–282, Mar. 2011.

[124] M. Pervaiz, S. Panthapulakkal, B. KC, M. Sain, and J. Tjong, "Emerging trends in automotive lightweighting through novel composite materials," *Materials Sciences and Applications*, vol. 07, no. 01, pp. 26–38, 2016.

[125] J. O'Keeffe. (2012) Composite enclosures combine light weight with shielding effectiveness. TE Connectivity. [Online]. Available: http://www.te.com/content/dam/te-com/documents/aerospace-defense-and-marine/white-papers/okeefe-composite-enclosures-combine-light-weight-shielding.pdf

John Reimers (IEEE S'16) received the B.Eng. degree in electrical engineering from McMaster University, Hamilton, Ontario, Canada in 2016, where he is currently working toward the Ph.D. degree with the McMaster Institute for Automotive Research and Technology (MacAUTO). He previously led a student team in the development and implementation of a hybrid-electric powertrain for an advanced vehicle technology competition. His research interests include power electronics and motor drives for electrified transportation applications.

Lea Dorn-Gomba (IEEE S'15) received the M.Eng. degree in electrical engineering from Ecole Nationale Superieure d'Electricite et de Mecanique (ENSEM), Nancy, France, in 2014, and the Ph.D. degree in electrical engineering from McMaster University, Hamilton, Canada, in 2018. She is currently working as a Postdoctoral Research Fellow with McMaster Automotive Resource Centre (MARC), McMaster University. Her research interests include design and control of power electronics, electrified transportation, and vehicle simulation modeling.

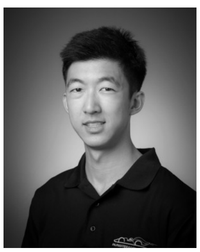

Christopher Mak received the B.Tech degree in Automotive Technologies from McMaster University, Hamilton, Ontario, Canada in 2016. Currently he is completing his M.A.Sc. degree in electrical engineering at McMaster University. He has been engaged in the development of electric machines and mechanical design.

Ali Emadi (IEEE S'98-M'00-SM'03-F'13) received the B.S. and M.S. degrees in electrical engineering with highest distinction from Sharif University of Technology, Tehran, Iran, in 1995 and 1997, respectively, and the Ph.D. degree in electrical engineering from Texas A&M University, College Station, TX, USA, in 2000. He is the Canada Excellence Research Chair Laureate at McMaster University in Hamilton, Ontario, Canada. He is also the holder of the NSERC/FCA Industrial Research Chair in Electrified Powertrains and Tier I Canada Research Chair in Transportation Electrification and Smart Mobility. Before joining McMaster University, Dr. Emadi was the Harris Perlstein Endowed Chair Professor of Engineering and Director of the Electric Power and Power Electronics Center and Grainger Laboratories at Illinois Institute of Technology in Chicago, where he established research and teaching facilities as well as courses in power electronics, motor drives, and vehicular power systems. He was the Founder, Chairman, and President of Hybrid Electric Vehicle Technologies, Inc. (HEVT) – a university spin-off company of Illinois Tech. Dr. Emadi has been the recipient of numerous awards and recognitions. He was the advisor for the Formula Hybrid Teams at Illinois Tech and McMaster University, which won the GM Best Engineered Hybrid System Award at the 2010, 2013, and 2015 competitions. He is the principal author/coauthor of over 450 journal and conference papers as well as several books including *Vehicular Electric Power Systems* (2003), *Energy Efficient Electric Motors* (2004), *Uninterruptible Power Supplies and Active Filters* (2004), *Modern Electric, Hybrid Electric, and Fuel Cell Vehicles* (2nd ed, 2009), and *Integrated Power Electronic Converters and Digital Control* (2009). He is also the editor of the *Handbook of Automotive Power Electronics and Motor Drives* (2005) and *Advanced Electric Drive Vehicles* (2014). He is the co-editor of *Switched Reluctance Motor Drives* (2018). Dr. Emadi was the Inaugural General Chair of the 2012 IEEE Transportation Electrification Conference and Expo (ITEC) and has chaired several IEEE and SAE conferences in the areas of vehicle power and propulsion. He is the founding Editor-in-Chief of the *IEEE Transactions on Transportation Electrification*.